

Cambridge University Press

978-1-558-99693-9 - Solid State Ionics-2002

Philippe Knauth, Jean-Marie Tarascon, Enrico Traversa and Harry L. Tuller

Excerpt

[More information](#)

Theory/Inorganic Ion Conductors

Cambridge University Press

978-1-558-99693-9 - Solid State Ionics-2002

Philippe Knauth, Jean-Marie Tarascon, Enrico Traversa and Harry L. Tuller

Excerpt

[More information](#)

Cambridge University Press

978-1-558-99693-9 - Solid State Ionics-2002

Philippe Knauth, Jean-Marie Tarascon, Enrico Traversa and Harry L. Tuller

Excerpt

[More information](#)

Mat. Res. Soc. Symp. Proc. Vol. 756 © 2003 Materials Research Society

EE1.1

THE *MIGRATION* CONCEPT FOR IONIC MOTION IN MATERIALS WITH DISORDERED STRUCTURES

K. FUNKE and R.D. BANHATTI

University of Münster, Institute of Physical Chemistry and Sonderforschungsbereich 458,
Schlossplatz 4, D – 48149 Münster, GermanyE-mail: K.Funke@uni-muenster.de and banhatt@uni-muenster.de

ABSTRACT

The dynamics of the mobile ions in materials with disordered structures are a challengingly complicated many-particle process. In this paper, we consider characteristic frequency-dependent conductivities and permittivities of such materials and show that they can be well reproduced within the framework of the *MIGRATION* concept. The meaning of the acronym is Mismatch Generated Relaxation for the Accommodation and Transport of IONs. In the *MIGRATION* concept, we attempt to grasp the essence of the ion dynamics in a simple set of rules which convey a physical picture of the most relevant elementary processes. The rules are expressed in terms of three coupled rate equations which then form the basis for deriving frequency-dependent model conductivities and permittivities.

I INTRODUCTION

Ion conducting materials with disordered structures comprise glasses as well as structurally disordered crystalline electrolytes. The frequency-dependent electric and dielectric properties of such materials are determined by the hopping dynamics of the mobile ions. Therefore, valuable information on the elementary hopping processes and, in particular, on correlations between hops are obtainable from a study of the frequency-dependent conductivity [1], $\sigma(\omega)$, and the (relative) frequency-dependent permittivity, $\varepsilon(\omega)$. The two functions are the constituent parts of the complex conductivity, $\hat{\sigma}(\omega) = \sigma(\omega) + i\omega\varepsilon_0\varepsilon(\omega)$. Here, ω denotes the angular frequency, while ε_0 is the permittivity of free space.

In the following, we consider data only below microwave frequencies, i.e., in a frequency range where $\sigma(\omega)$ has to be attributed entirely to the hopping motion of the ions, while vibrational contributions to $\sigma(\omega)$ may still be neglected. In this frequency range, vibrations and fast ionic polarizations as well as even faster (electronic) processes contribute a constant value, $\varepsilon(\infty)$, to $\varepsilon(\omega)$, while the remaining part, $\varepsilon(\omega) - \varepsilon(\infty)$, results from the hopping motion. Sometimes, we will use the notation $\hat{\sigma}_{HOP}(\omega) = \hat{\sigma}(\omega) - i\omega\varepsilon_0\varepsilon(\infty)$.

A surprising experimental observation is made when conductivity spectra, $\sigma(\omega)$, of different fast ion conducting materials, i.e. of structurally disordered crystals and glassy

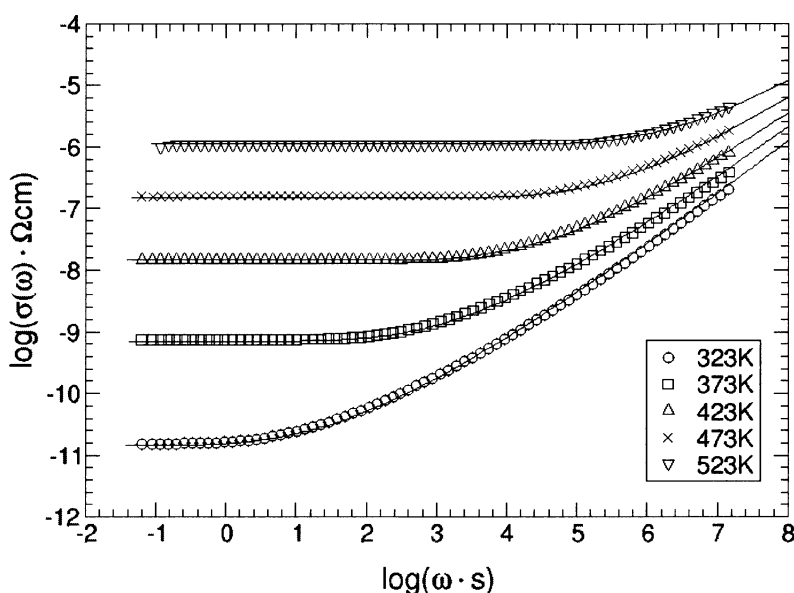


Fig. 1a: Conductivity isotherms of $0.2\text{Na}_2\text{O} \cdot 0.8\text{GeO}_2$ glass. Fits are made using the CMR model (Eq.(9)).

electrolytes, are compared with each other. In fact, many of them are found to be virtually identical in shape, not only for a given material at different temperatures, but even for different materials. This is most clearly seen when a *scaled* conductivity is plotted versus a *scaled* angular frequency. This property of scaling is known as the time-temperature superposition principle [2-12]. In our notation, $\sigma_s(\omega_s)$, the scaled conductivity is meant to be $\sigma_s(\omega) = \sigma(\omega)/\sigma(0)$, and the scaled angular frequency is $\omega_s = \omega/\omega_0$. Here, ω_0 marks the onset of the conductivity dispersion on the ω scale. A quantitative definition will be given later, see Eq. (12).

Figures 1a and 1b are, respectively, plots of unscaled and scaled ionic conductivities of a particular glassy ion conductor, namely, a sodium germanate glass of composition $0.2\text{Na}_2\text{O} \cdot 0.8\text{GeO}_2$ [8,13]. Virtually the same scaled curve, $\sigma_s(\omega_s)$, as in Fig. 1b has also been obtained for many other glassy and crystalline fast ion conductors [2-12]. Therefore, this “master curve” must be considered representative.

Recently, a model concept has been introduced which is able to explain experimental data such as those of Fig. 1 on the basis of two simple coupled rate equations. The model rate equations are meant to grasp the essence of the rules that determine the dynamics of the mobile ions. This model, called the concept of mismatch and relaxation (CMR) [14], will be outlined in section III. In fact, the solid lines in Figs. 1a and 1b, which reproduce the experimental conductivities very well, have been derived from the CMR.

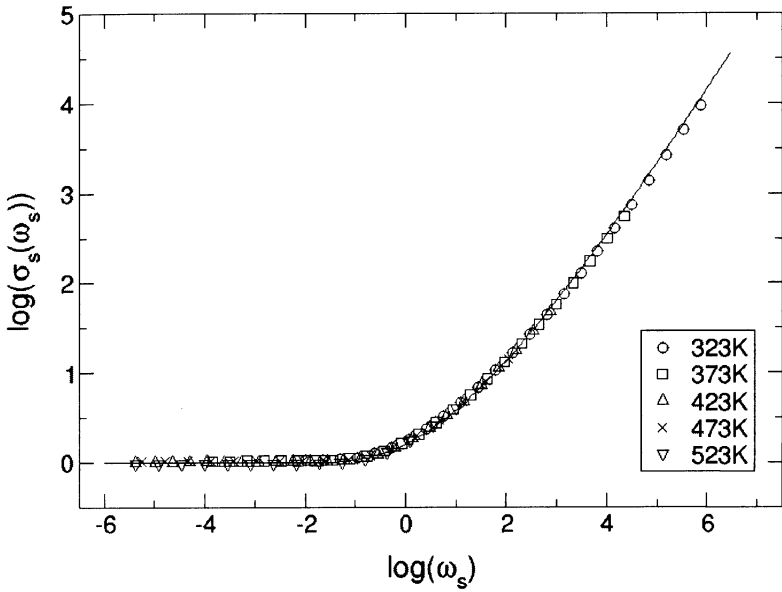


Fig. 1b: Scaled conductivity plot for 0.2 Na₂O · 0.8 GeO₂ glass. Fit using the CMR model with exponent K=2 (see Eq.(10)).

The main purpose of the present contribution is, however, to extend our model treatment to include also the frequency dependence of the permittivity, $\epsilon(\omega)$. As will be shown in sections II and IV, it is useful to introduce and discuss a scaled version of this function, $\epsilon_s(\omega_s)$, in analogy to $\sigma_s(\omega_s)$. In section IV, we will further see that the extreme long-time/low-frequency behavior inherent in the CMR does not match the low-frequency behavior of $\epsilon(\omega)$ and, in particular, does not reproduce its dc plateau, $\epsilon(0)$. Therefore, we have to reformulate our model. We do so by suggesting a subtle change which has a clear physical meaning and becomes significant only at long times. This change hardly affects the results obtained for $\sigma(\omega)$ and $\sigma_s(\omega_s)$, but yields the proper long-time behavior determining the shape of $\epsilon(\omega)$ at low frequencies.

At the advanced stage to be presented in section IV, our model is called the MIGRATION concept, the acronym standing for Mismatch Generated Relaxation for the Accommodation and Transport of IONs. In the MIGRATION concept, the dynamics of the mobile ions are described in terms of three coupled rate equations (instead of two in the CMR). Experimental spectra, $\sigma(\omega)$ and $\epsilon(\omega)$, as well as the scaled functions, $\sigma_s(\omega_s)$ and $\epsilon_s(\omega_s)$, are well reproduced by the MIGRATION concept.

This paper is organized as follows. In section II, the time-dependent correlation factor, $W(t)$ [15], is introduced in order to provide an effective means to express both unscaled and scaled conductivities and permittivities. In section III, $W(t)$ is obtained from the CMR rate

equations and then used to construct frequency-dependent conductivities such as those of Figs. 1a and 1b. Eventually, section IV is devoted to a discussion of the shape of frequency-dependent permittivities and to the formulation of the MIGRATION concept.

II SCALED CONDUCTIVITIES AND PERMITTIVITIES

The complex conductivity, $\hat{\sigma}_{HOP}(\omega)$, is proportional to the Fourier transform of the autocorrelation function of the current density due to the hopping [16], which is a real function of time:

$$\hat{\sigma}_{HOP}(\omega) \propto \int_0^{\infty} \langle \vec{i}(0) \cdot \vec{i}(t) \rangle_{HOP} \cdot \exp(-i\omega t) \cdot dt. \quad (1)$$

The current density itself,

$$\vec{i}(t) = \frac{q}{V} \sum_{i=1}^N \vec{v}_i(t), \quad (2)$$

is proportional to the ionic charge, q , inversely proportional to the volume of the sample, V , and proportional to the sum of the velocities of the mobile ions, $\vec{v}_i(t)$. Therefore, its autocorrelation function contains a large number of cross terms, $\langle \vec{v}_i(0) \cdot \vec{v}_j(t) \rangle$, with $i \neq j$. In our treatment we, however, assume that their role is negligible, which implies that the Haven ratio, i.e., the factor in the Nernst-Einstein relation, is close to unity [17]. In this case, $\hat{\sigma}_{HOP}(\omega)$ will be proportional to the Fourier transform of the velocity autocorrelation function, $\langle \vec{v}(0) \cdot \vec{v}(t) \rangle_{HOP}$. In order to derive realistic conductivity spectra, we have to envisage a shape of this function as schematically outlined in Fig. 2.

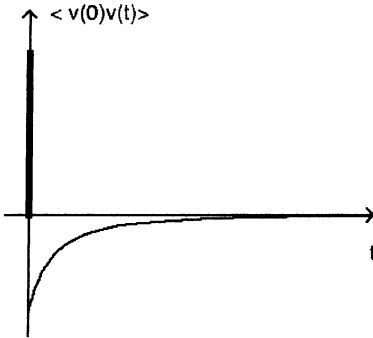


Fig.2: Schematic representation of the velocity autocorrelation function.

Cambridge University Press

978-1-558-99693-9 - Solid State Ionics-2002

Philippe Knauth, Jean-Marie Tarascon, Enrico Traversa and Harry L. Tuller

Excerpt

[More information](#)

The intense narrow component at very short times corresponds to the velocity autocorrelation during one single hop, while the decaying negative component at longer times results from a decaying probability for a correlated “backward” hop to occur after the “initial forward” hop. The time-dependent correlation factor, $W(t)$, which is now introduced, is the normalized integral of $\langle \vec{v}(0) \cdot \vec{v}(t) \rangle_{HOP}$, with $W(0)=1$. At long times, $W(t)$ tends to $W(\infty)$. This value, $W(\infty)$, is the fraction of “successful” hops. While all hops contribute to the ionic conductivity at sufficiently high frequencies, i.e., in the high-frequency plateau, $\sigma = \sigma(\infty)$, only the successful ones contribute to the conductivity at low frequencies, i.e., in the low-frequency plateau, $\sigma = \sigma(0)$. Note that the high-frequency plateau is not included in Figs. 1a and 1b.

The relationship between $\hat{\sigma}_{HOP}(\omega)$ and $W(t)$ is then

$$\frac{\hat{\sigma}_{HOP}(\omega)}{\sigma(\infty)} = 1 + \int_0^{\infty} \dot{W}(t) \cdot \exp(-i\omega t) \cdot dt, \quad (3)$$

where the dot denotes a differentiation with respect to time.

In view of experimental data such as those of Fig. 1, it is advantageous to formulate the ratio, $\hat{\sigma}_{HOP}(\omega)/\sigma(0)$, which we call $\hat{\sigma}_s(\omega)$, in terms of $W(t)$ or, rather, in terms of the scaled correlation factor, $W_s(t) = W(t)/W(\infty)$:

$$\hat{\sigma}_s(\omega) = W_s(0) + \int_0^{\infty} \dot{W}_s(t) \cdot \exp(-i\omega t) \cdot dt. \quad (4)$$

After replacing $\dot{W}_s(t)$ with $d(W_s(t)-1)/dt$, integration by parts yields

$$\hat{\sigma}_s(\omega) = 1 + i\omega \int_0^{\infty} (W_s(t)-1) \cdot \exp(-i\omega t) \cdot dt. \quad (5)$$

Introducing scaled times and angular frequencies via $t_s = t/t_0$ and $\omega_s = \omega/\omega_0$, with t_0 and $\omega_0 = 1/t_0$ to be defined in the next section, we find for the real part of Eq. (5):

$$\sigma_s(\omega_s) = 1 + \omega_s \int_0^{\infty} (W_s(t_s)-1) \cdot \sin(\omega_s t_s) \cdot dt_s. \quad (6)$$

The experimental observation of scaling, cf. Fig. 1b, means that variations of $W_s(t_s)$ with temperature or with the material under consideration have only negligible influence on $\sigma_s(\omega_s)$. This is a remarkable statement.

In a second step, we consider a scaled permittivity,

$$\epsilon_s(\omega_s) = \text{Im} \hat{\sigma}_s(\omega_s) / \omega_s = \frac{\epsilon_0 \omega_0}{\sigma(0)} \cdot (\epsilon(\omega_s) - \epsilon(\infty)). \quad (7)$$

From the imaginary part of Eq. (5), $\epsilon_s(\omega_s)$ is found to be

$$\epsilon_s(\omega_s) = \int_0^\infty (W_s(t_s) - 1) \cdot \cos(\omega_s t_s) \cdot dt_s. \quad (8)$$

In a formal sense, Eq. (8) is similar to Eq. (6). The question, however, of whether or not $\epsilon_s(\omega_s)$ will also display the property of scaling, is not easy to answer *a priori* from Eq. (8), since the temperature dependence of $W_s(t_s)$ at short scaled times will have much more effect on the cosine transform of Eq. (8) than on the sine transform of Eq. (6).

In this section, the problem of reproducing experimental (unscaled and scaled) conductivity and permittivity spectra has been reduced to the problem of finding a realistic scaled correlation factor, $W_s(t_s)$.

III THE CMR AND SCALED CONDUCTIVITY

The solid line included in Fig. 1b, which reproduces the scaled conductivity spectrum very well, has been calculated from Eqs. (9) and (6). Equation (9) is a rate equation for $W_s(t_s)$:

$$-\frac{dW_s(t_s)}{dt_s} = (W_s(t_s) \cdot \ln W_s(t_s))^2. \quad (9)$$

It results from the CMR rate equations [14],

$$-\dot{g}(t) = A \cdot g^2(t) \cdot W(t) \quad (10)$$

$$-\dot{W}(t) = -B \cdot \dot{g}(t) \cdot W(t), \quad (11)$$

and from the definition of t_s , see Eq. (13) below.

In Eqs. (10) and (11), $g(t)$ is a normalized mismatch function, see [14,15], while A and B are temperature-dependent constants. Suppose an ion (the “central” ion) performs a hop from site X to site Y at time $t = 0$. It thereby creates mismatch between its own position and the position where it would be optimally relaxed with respect to the arrangement of its neighbors.

Cambridge University Press

978-1-558-99693-9 - Solid State Ionics-2002

Philippe Knauth, Jean-Marie Tarascon, Enrico Traversa and Harry L. Tuller

Excerpt

[More information](#)

In Eqs. (10) and (11) we then consider a later time, $t > 0$, and assume that the ion is now (still or again) at site Y, which is the case with probability $W(t)$. In this situation, we observe the system reducing its mismatch. This is possible either on the single-particle route, with the ion hopping back to X, or on the many-particle route, with the mobile neighbors rearranging. Equation (11) claims that the rates on these routes, $-\dot{W}(t)/W(t)$ and $-g(t)$, respectively, are proportional to each other at all times. The function $g(t)$ decays from $g(0)=1$ to $g(\infty)=0$, while $W(t)$ decays from $W(0)=1$ to $W(\infty)=\exp(-B)$. Equation (11) implies that $1+(\ln W(t))/B$ and $g(t)$ are identical at all times.

The other equation, Eq. (10), describes the decay of $g(t)$ on the many-particle route. Here it is useful to regard $g(t)$ as a normalized electric dipole moment. Its dipole field influences the hopping motion of the other mobile ions in the neighborhood, facilitating hops in their respective preferred directions. This has two consequences, which are both included in Eq. (10). In the first place, $g(t)$ will decay with time and, secondly, the dipole field becomes increasingly shielded. The rate of reduction of g at time t is proportional to the convolution of the driving force, which is g itself, and the velocity autocorrelation function of the neighboring ions. The latter function is assumed to be the same as for the “central” ion. Apart from a normalization factor, the product $g(t) \cdot W(t)$ turns out to be an excellent approximation for this convolution. The progressive shielding is taken into account by a time-dependent effective number, $N(t)$, of neighboring mobile ions which at time t still experience the dipole field. Then Eq. (10) results from the empirical, yet plausible assumption that $N(t)$ is itself proportional to $g(t)$.

Equation (9) is obtained from Eqs. (10) and (11) in two steps. In the first step, $g(t)$ is eliminated. The resulting function $W(t)$ allows us to reproduce unscaled conductivity spectra such as those of Fig. 1a via Eq. (3). In the second step, we define an onset angular frequency of the conductivity dispersion, ω_0 , by

$$\omega_0 = \frac{A}{B} \cdot \exp(-B). \quad (12)$$

The inverse of the onset angular frequency, $t_0 = 1/\omega_0$, may be regarded as the time at which the hopping motion of the ions becomes random. The scaled time used in Eq. (9) is then

$$t_s = \frac{t}{t_0} = t \cdot \omega_0. \quad (13)$$

Although examples have been found where the exponent K in Eq. (10) differs from two, cf. Refs. [14,18], these are not considered in this paper. Rather, we focus on those numerous glassy and crystalline electrolytes for which the exponent K is two.

The remarkable result of this section consists in having found a unique function $W_s(t_s)$ and, therefore, a unique function $\sigma_s(\omega_s)$, which is indeed in good agreement with the experimental data of many ion-conducting materials, cf. the characteristic example of Fig. 1.

Cambridge University Press

978-1-558-99693-9 - Solid State Ionics-2002

Philippe Knauth, Jean-Marie Tarascon, Enrico Traversa and Harry L. Tuller

Excerpt

[More information](#)

In order to transform the spectra of Fig. 1a into the scaled spectrum of Fig. 1b, the ω axis has been replaced by an ω/ω_0 axis, with $\omega_0 = (A/B) \cdot \exp(-B)$. It is interesting to note that this scaling is equivalent to the so-called Summerfeld scaling [19] where, apart from a constant, the product, $T \cdot \sigma(0)$, is used for normalizing the ω scale. The reason for the equivalence is as follows. Comparing model conductivity isotherms and experimental ones [14], we always find $A \propto \sigma(\infty)$ and, as a consequence, $A \cdot \exp(-B) \propto \sigma(0)$. Since both $\sigma(\infty)$ and $\sigma(0)$ are Arrhenius activated, the same holds true for $\sigma(0)/\sigma(\infty) = \exp(-B)$, which implies $1/B \propto T$. Therefore, forming $\omega_0 = (A/B) \cdot \exp(-B)$, we now realize that $\omega_0 \propto T \cdot \sigma(0)$ must hold, which means that our model scaling and the Summerfeld scaling are equivalent. In either case, the basic assumption is that the only effect of temperature is to speed up or slow down the ionic hopping processes, while the underlying mechanism remains unchanged.

IV THE MIGRATION CONCEPT AND SCALED PERMITTIVITY

In Fig. 3a, we present frequency-dependent permittivities, $\epsilon(\omega)$, of the glassy electrolyte $0.2\text{Na}_2\text{O} \cdot 0.8\text{GeO}_2$ at different temperatures. These correspond to the conductivities of Fig. 1a. Likewise, Fig. 3b is a plot of the scaled permittivity of this system, $\epsilon_s(\omega_s)$, as constructed from the experimental data of Fig. 3a via Eq. (7). Figure 3b thus corresponds to the scaled conductivity of Fig. 1b. However, Fig. 3b should not be taken as "representative" for all materials (see below).

At this stage, two statements can be made. In the first place we note that, in the scaled representation of Fig. 3b, the permittivity data do, indeed, superimpose. Secondly, we see that $\epsilon_s(\omega_s)$ has a temperature-independent, finite low-frequency value, $\epsilon_s(0)$.

The solid lines included in Figs. 3a and 3b have been obtained from the MIGRATION concept, which will be presented in this section.

The necessity to replace the CMR with a more appropriate treatment, i.e. with the MIGRATION concept, arises from the following observation. Trying to explain the data of Figs. 3a and 3b on the basis of the CMR equations, Eqs. (10) and (11), we encounter a problem. In the extreme long-time limit, when $W(t)$ approaches $W(\infty)$ asymptotically, we find from these equations that both $-\dot{g}$ and $-\dot{W}$ vary with time as $1/t$. Inserting the proportionality, $-\dot{W}_s \propto 1/t$, into Eq. (4) and considering the imaginary part of this equation, we find that $\epsilon(\omega)$, in the limit of $\omega \rightarrow 0$, diverges logarithmically, in disagreement with experimental results, which clearly prove that $\epsilon(0)$ is finite. Therefore, Eqs. (10), (11) cannot be correct in the long-time limit.

The puzzle can be solved by a more careful and physically more realistic choice of the number function, $N(t)$, in the limit of long times. As outlined in the previous section, Eq. (10) is based on the idea that

$$-\frac{\dot{g}(t)}{g(t)} \propto W(t) \cdot N(t). \quad (14)$$